The development of in vivo confocal laser scanning microscopy in the late 1980s permitted precise three-dimensional (3D) visualization of microstructures of the ocular fundus in particular, with its optic nerve head and the peripapillary retina [75, 93]. Modern digital image processing technology enables quantitative data to be collected noninvasively, rapidly, and with a low level of illumination. The precision of laser scanning ophthalmoscopy in this context is based on the principle of the confocality of the examined object with the light source and the detector plane. A laser light source is focused through a pinhole diaphragm to one point on the object. The reflected laser light is separated by a beam splitter from the incident laser beam path and is deflected through a second confocal diaphragm to reach a photosensitive detector. Because of the confocal design, light originating from outside the focal plane is highly suppressed, and only the object layer located at the focal plane contributes to the image. To build up a two-dimensional (2D) image perpendicular to the optical axis of the device, the laser beam has to scan the sample point by point. This is achieved by introducing two oscillating mirrors into the beam path. Figure 2.1 provides a schematic illustration of this principle. By optical movement of the focal plane, an image can be acquired from a deeper layer of the examined object, thus enabling a data cube to be built up in a successive series.

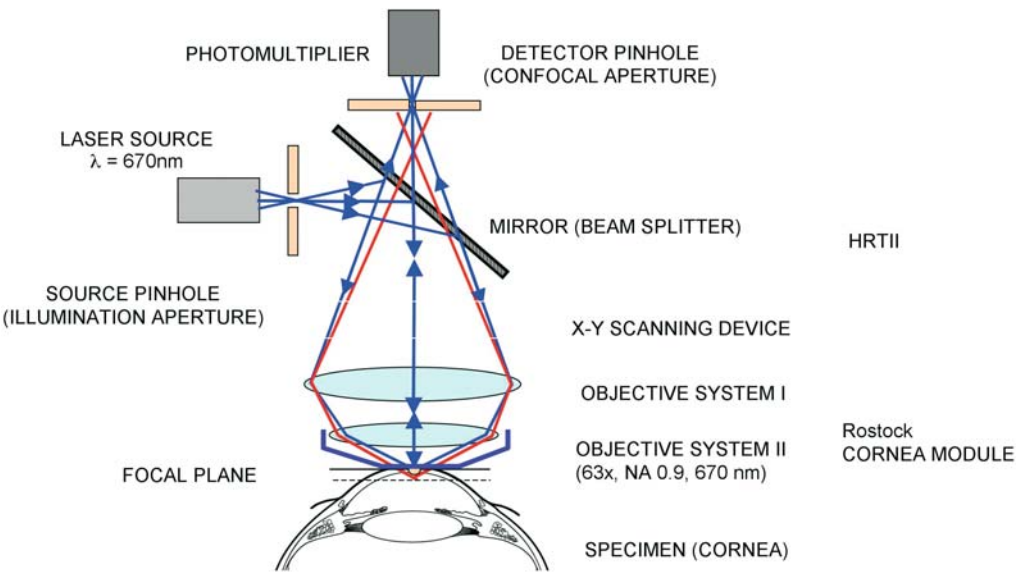

Fig. 2.1 Principle of confocal laser-scanning microscopy

In contrast, in slit-lamp biomicroscopy examination of the cornea, an optical section that is essentially perpendicular to the corneal surface is seen in up to ×50 magnification or, with an additional lens for endothelial viewing (specular microscopy), in up to ×200 magnification. Nowadays, documentation is generally performed using digital photography. All other cellular structures, such as the epithelium, cannot be imaged with this technique because of the high proportion of scattered light.

Optical tomography perpendicular to the incident light path has become possible only with the adaptation of confocal microscopy, as described above, for examining the living eye [7, 11, 12, 37, 55, 86, 87]. This yields images of the endothelium, for example, that are comparable to those obtained with specular microscopy. In this case, the most pronounced source of scattered light is the cytosol of the endothelial cells, with the result that the cell borders appear dark. Only light reflected from the focal plane contributes to the image. In this way, cell structures in the stroma, nerves, and corneal epithelium [95] can also be imaged in fine optical sections.

Fig. 2.2 Confocal slit-scanning microscope (ConfoScan 3; Nidek Technologies, Vigonza, Italy)

2.1 Slit-Scanning Techniques

Techniques based on the principles of the rotating Nipkow disk or tandem slit-scanning were used initially for confocal microscopy of the anterior segment of the eye. Figure 2.2 shows a slit-scanning microscope of this type that incorporates the use of a halogen lamp. For corneal assessment these microscopes can be used to image confocal sections with an optical layer thickness of approximately 5–10 µm. Synchronization of slit-scanning [47, 86, 94] with the video rate of a residual light camera yields sharp and motion-independent image sequences at 25 frames per second [46, 48] (Fig. 2.3).

Three-dimensional image distortion due to eye movements with this noncontact microscopy technique can be minimized only by faster image acquisition. However, more rapid movement of the confocal plane along the optical axis (*z*-scan) is accompanied by a loss of resolution. Loose optical coupling to the cornea using a gel (Fig. 2.4) limits the precision of depth information relating to the optical section in the cornea and, hence, the 3D reconstruction of cell structures [57, 65, 78]. Systematic errors such as inhomogeneous image illumination and image distortion also arise as a result of the electromechanical slit-scanning technique used. Linear movement along the *z*-axis during individual image acquisition also produces distortion along the *z*-axis. These fundamental sources of error can be prevented only by a rapid laser scanning system unhampered by mass inertia and incorporating a serial dot-raster technique with stepwise advance of the confocal plane during the *z*-scan.

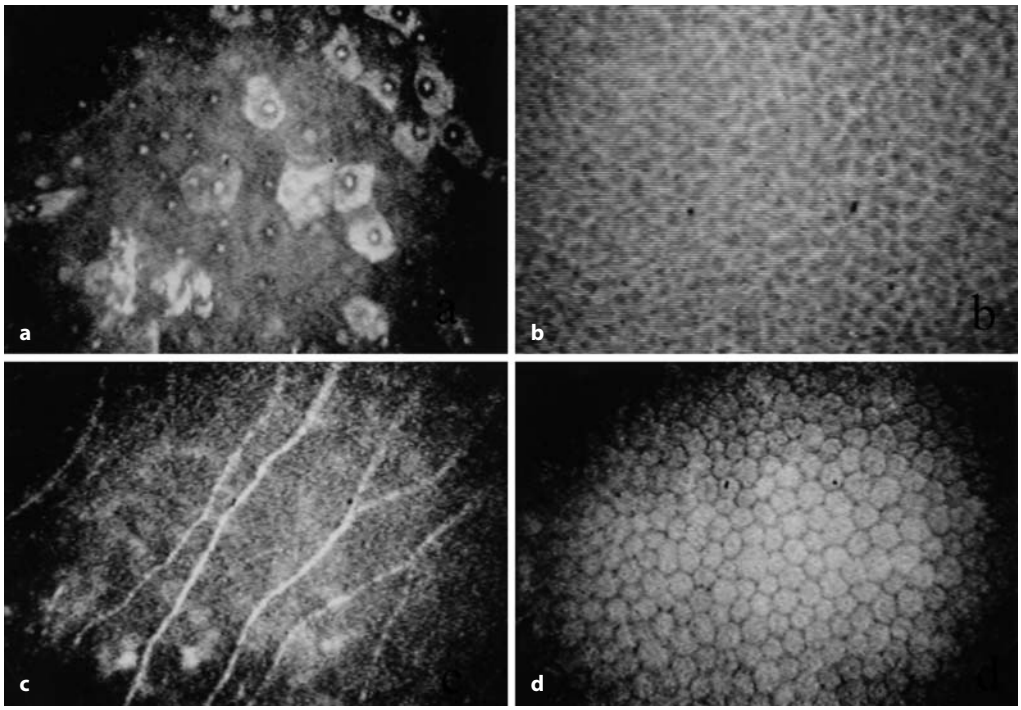

Fig. 2.3 Slit-scanning microscopy. **a** Superficial cells. **b** Basal cells. **c** Nerve plexus with keratocytes and (**d**) endothelium

Fig. 2.4 Gel coupling between lens and eye (ConfoScan 3; Nidek Technologies, Vigonza, Italy)

2.2 Laser Scanning Imaging Plus Pachymetry

As an alternative to confocal slit-scanning microscopes, a confocal laser scanning microscope for the anterior segment of the eye was developed at the Rostock Eye Clinic (Germany) on the basis of an already commercially available laser scanning system. Not least because of its compact construction, the Heidelberg Retina Tomograph II (HRT II, Heidelberg Engineering, Germany) was selected as the basic device for a digital confocal corneal laser scanning microscope.

In laser scanning ophthalmoscopy of the posterior segment, the optically refractive media of the eye form part of the optical imaging system. For anterior segment applications, a high-quality microscope lens is positioned between the eye and the device, providing a laser focus less than 1 µm in diameter. The result is a

Fig. 2.5 Rostock Cornea Module (RCM; confocal laser scanning microscope). **a** Feasibility study of the fully automated control of the microscope using a separate personal computer, step motors (*x*-, *y*-, *z*-scan), and joystick. **b** RCM (contact) and digital camera

high-resolution, high-speed, digital confocal laser scanning microscope that permits in vivo investigation of the cornea (Fig. 2.5). Movement of the confocal image plane inside the cornea can be achieved manually at the microscope lens or by using the automatic internal *z*-scan function of the HRT II. Laser scanning tomography is consequently possible in the anterior segment of the eye.

This technique permits rapid and reliable visualization and evaluation of all the microstructures in the cornea, including the epithelium, nerves, and keratocytes, as well as the endothelium and bulbar conjunctiva. For the first time, the dendritic (or Langerhans) cells can now also be visualized in vivo with an image quality that permits quantification [83, 97]. In principle, any body surface that can be reached by the lens system is a suitable candidate for examination, with the result that potential applications also exist outside ophthalmology (for instance, for the skin, tongue surface, and oral mucosae).

The original functions of the basic HRT II device for evaluating the optic nerve head in glaucoma are fully retained when the system is modified into the confocal laser microscope. Software adapted to the special requirements of scanning microscopy of the cornea has also been developed. This software permits the acquisition of individual section images, image sequences of section images, and volume images with internal *z*-scan over a distance of approximately 80 µm. The digital properties of the device offer good patient and image data administration and also deliver rapid access to – and hence comparison with – data from previous examinations.

The HRT II has been modified with a lens system attachment known as the Rostock Cornea Module (RCM; J. Stave, utility model number 296 19 361.5, licensed to Heidelberg Engineering, Germany). The module is combined with a manual *z*-axis drive to move the focal plane inside the cornea. This enables a cell layer at any depth to be imaged and, for example, selected as the starting plane for the automated internal *z*-scan. During the examination, pressure-free and centered contact with the cornea can be monitored visually using a color camera.

The distance from the cornea to the microscope is kept stable by use of a single-use contact element in sterile packaging (TomoCap®). Optical coupling is achieved via the tear film or protective gel to the eye. The TomoCap® is a thin cap with a planar contact surface made from polymethyl methacrylate (PMMA) and is coupled optically to the lens with the aid of a gel. Special caps with small tips have been developed for experimental animal work in rats and rabbits (Fig. 2.6).

Confocal laser scanning microscopy attempts to register the reflected laser beam and the intrinsic beam of reflection microscopy and fluorescence microscopy at a very low level, even in thick tissue specimens, using objectives with a high numerical aperture. As a rule, these

Fig. 2.6 TomoCap® contact cap (Rostock Cornea Module). **a** TomoCap®. **b, c** Special caps for animal experiments. **d** Cap with a depression in the cap front. **e** Prismatic cap for slant imaging of the cornea

are immersion objectives. The resolution of a microscope is determined using the following equation:

$$R = 0.61\lambda/NA$$

(R = resolution, λ = wavelength, NA = numerical aperture)

Accordingly, the spatial resolution of the objective used (Zeiss ×63/0.95 W, 670 nm, ∞/0, Jena, Germany) and of the carbomer contact gel (Vidisic; Dr.Mann Pharma, Berlin, Germany) with a refractive index of n=1.350 (water n=1.330) yields a value of

$$R = 0.61 \times 0.670/0.95 = 0.430\ \mu m$$

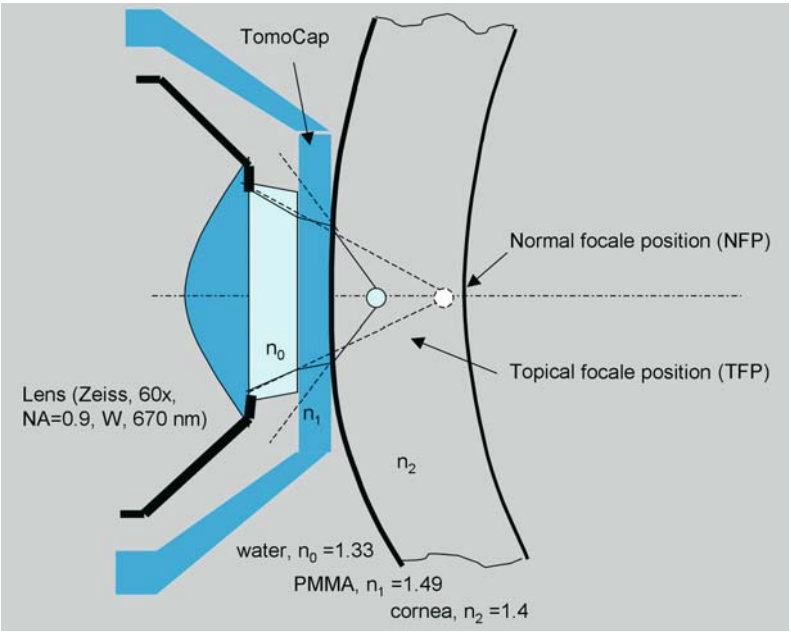

Fig. 2.7 Contact microscopy using the TomoCap® of the Rostock Cornea Module

Depth resolution in confocal microscopy is determined as a function of the available amount of light, the numerical aperture, and the sensible size of the detector diaphragm. In the case of the HRT II–RCM, the depth resolution is approximately 1–2 µm.

Figure 2.7 illustrates the coupling of the microscope to the cornea via the single-use PMMA contact element (Stave, GB 296 12 466.4/1996). As well as stabilizing the distance between the microscope and cornea, thus permitting exact depth data on the location of the optical section in the cornea (optic pachymetry), the higher refraction index of the PMMA cap material (n=1.49) produces an immersion structure in front of the cornea, which increases the numerical aperture and hence the resolution.

The numerical aperture can be calculated from the following equation:

$NA = n \sin\alpha$
(angle α = half the angle of aperture)

Accordingly, the limiting factor is the refractive index of the liquid contact medium used (Vidisic; n=1.350): Insertion of the PMMA contact disk of the TomoCap®, which is coupled to the objective using a liquid immersion medium, produces an immersion sandwich structure in front of the cornea. As the PMMA cap material, with the higher refractive index of n_1=1.490, moves into the cornea, with an average refractive index of n_2=1.44, there is a focus shift toward the contact plate due to refraction, according to Snellius' law. The consequences of this are increased numerical aperture and resolution and improved contrast.

Figure 2.8 shows the influence of the immersion medium on the numerical aperture of the objective.

In the case of homogeneous immersion, the refractive indices of the objective lens and the immersion fluid are made so similar for the key wavelength that the beams emitted from the object point pass unbroken through the immersion film and are thus taken up by the object lens. The result is a high light intensity that decisively determines the resolution.

In the special case involving coupling with the PMMA cap with a high refractive index, the numerical aperture is increased by the factor n_2, and thus the limit of resolution is reduced to $1/n_2$. Consequently, when the cap is used, the water-immersion objective (microscopy without the PMMA

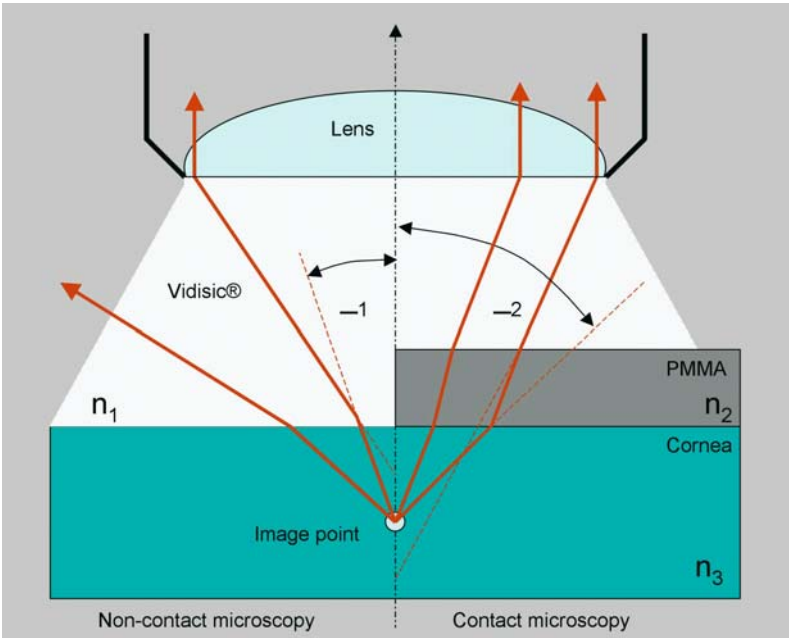

Fig. 2.8 Influence of the immersion medium on the numerical aperture of the lens

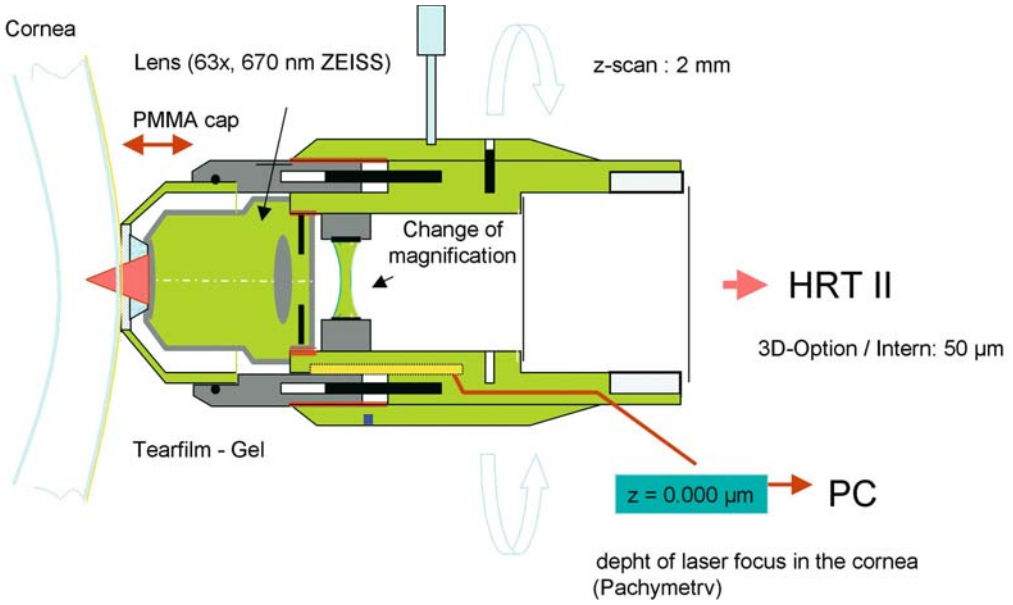

Fig. 2.9 Rostock Cornea Module (RCM)

cap) differs in terms of the numerical aperture by a factor of n_2=1.44, provided that beams can be taken up with the same angle of aperture.

In addition, the immersion layers avoid reflections at the interfaces.

In the 3D imaging mode, the distance between two subsequent image planes is approximately 2 µm in the cornea. A 3D image consists of 40 image planes, thus covering a depth range of 80 µm. The acquisition time for a volume image is 6 s, and each individual section image is recorded in 0.024 s. In the image sequence acquisition mode, up to 100 images can be stored with variable frame rates (1–30 frames per second). It thus becomes possible to document dynamic processes in the tissue (for example, blood flow in the sclera). When the RCM is used to set a plane manually at a desired depth, such as at the laser-assisted in situ keratomileusis (LASIK) interface after laser surgery to correct refraction, image series from this depth can be acquired with almost 100% image yield and precise depth allocation [43, 58, 59, 91].

With the HRT II, *z*-axis movement between images in the internal *z*-scan is performed – for the first time – in a stepwise manner; that is, during acquisition of one section image, the *z*-setting remains constant. This is a major advance and a prerequisite for generating distortion-free images of structure from one plane during the *z*-scan. A crucial prerequisite for undistorted 3D reconstructions has therefore been achieved [35].

A short focal length water-immersion microscope lens with a high numerical aperture was used to achieve high magnification (Achroplan ×63 W/NA 0.95/AA 2.00 mm, 670 nm, Carl Zeiss; alternatively, LUMPLFL ×60 W/NA 0.90/AA 2.00 mm, Olympus). To optimize image quality, the Zeiss microscope lens was customized with a special antireflection coating appropriate for the laser wavelength.

With the aid of an additional lens positioned between the HRT II and the microscope lens, the field of view of the scanning system (fixed at 15° with the HRT II) is reduced to approximately 7.5° to allow for the necessary magnification (Fig. 2.9). Depending on the microscope lens and additional lens used, the size of the field of view in the contact technique can be 250 µm ×

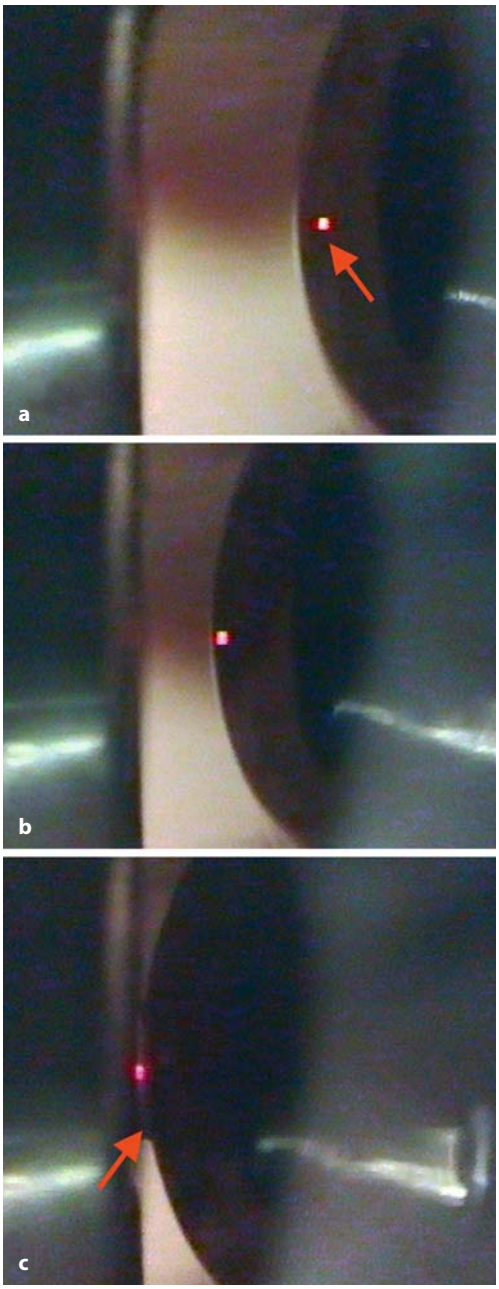

Fig. 2.10 Camera-controlled contact procedure: laser reflexes (*arrow*) on the cornea, producing the immersion gel bridge (*arrow*) between the objective lens/cap and the cornea (**a–c**)

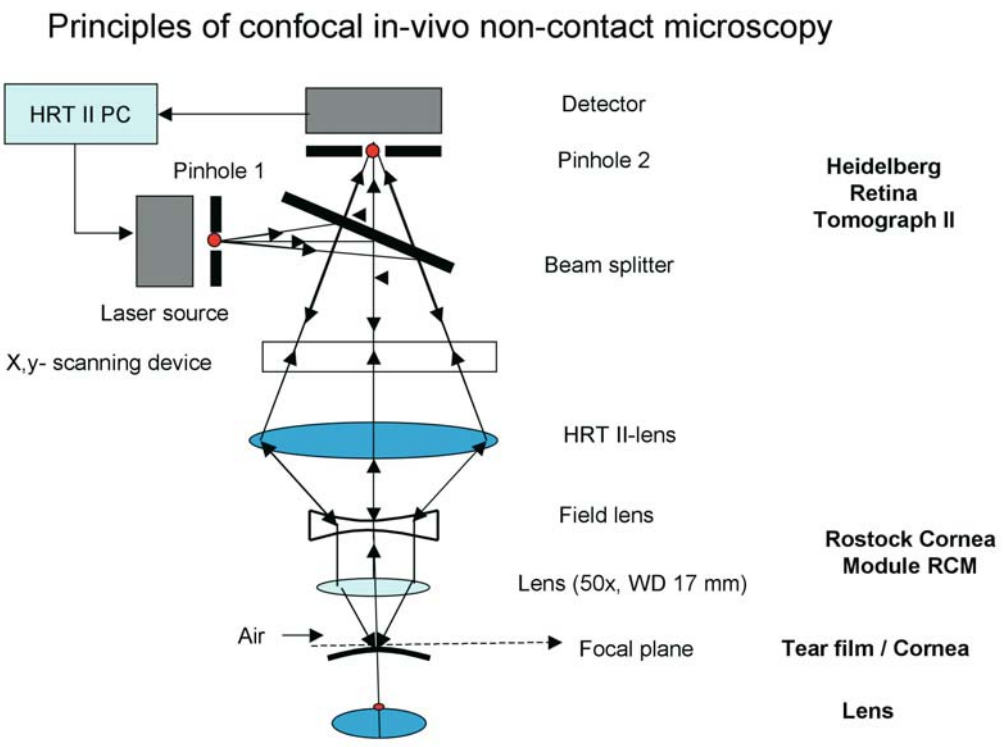

Fig. 2.11 Principles of confocal in vivo noncontact microscopy

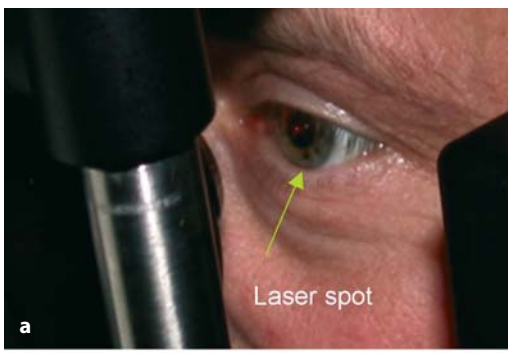

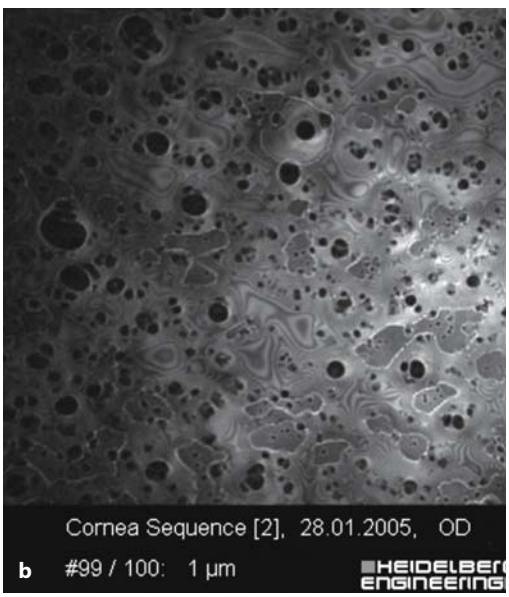

Fig. 2.12 Confocal in vivo noncontact microscopy. **a** Position of the laser light reflex in the center of the cornea during noncontact examination. **b** Example of a tear film image (ointment in the eye)

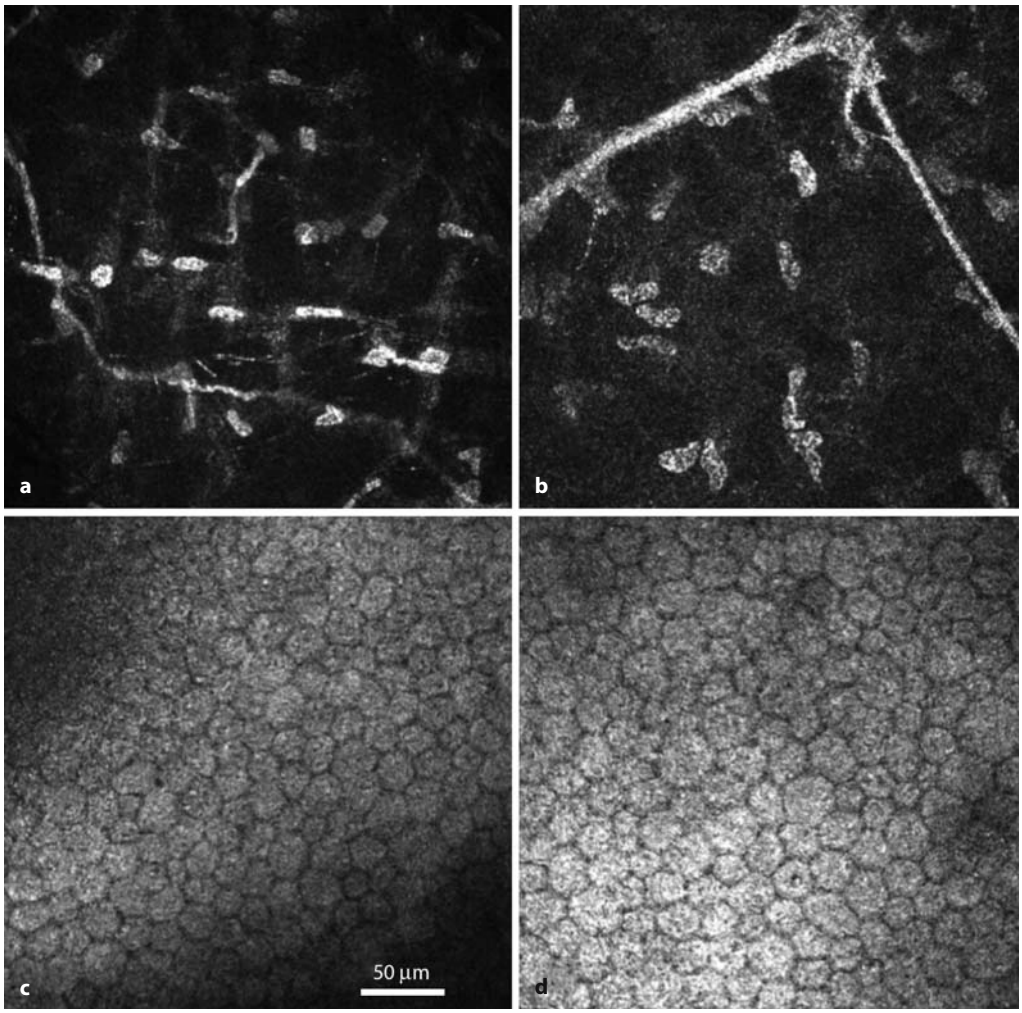

Fig. 2.13 Confocal in vivo noncontact microscopy: **a, b** Posterior stroma (keratocytes/nerve). **c, d** Endothelium

250 µm, 400 µm × 400 µm, or 500 µm × 500 µm. Dry microscope lenses can be used in noncontact work, such as to image the tear film [79].

In particular, the compact construction of the HRT II simplifies its use as a confocal in vivo microscope because the view is virtually unobscured when monitoring the patient and bringing the microscope up to the cornea.

The precise perpendicular positioning of the cornea in front of the microscope within the micrometer range is facilitated by color camera control. By observing the laser reflex on the cornea, even when bringing the microscope to the eye, the user can make a lateral or vertical correction so that contact with the cornea is exactly in the optical axis (Fig. 2.10 a–c). As a result, images are captured only of cell structures that are in a plane parallel to the surface; that is, transverse sectional images are acquired. The contact technique guarantees a fixed distance between the microscope and the cornea. The precise movement of the focal plane through the cornea with simultaneous digital recording of depth position relative to the superficial cells of the epithelium (at the corneal surface) thereby makes exact pachymetry possible (Figs. 2.11–2.13).

2.3 Basics of Image Formation in Confocal In Vivo Microscopy

The laser light that is emitted constitutes an electromagnetic wave with a defined wavelength lambda (λ). This light wave is modified when it passes through the cornea. Part of it migrates unchanged through all layers (transmission). At interfaces with changing refraction indices (n_D), the wave alters direction because of scatter and refraction. Light scattering is the basis of image formation in confocal microscopy in which only back-scattered light is used for the image. The amount of back-scattered light is very small because scatter occurs predominantly in a forward direction [18]. Light-scattering interfaces are found in the cornea, such as at the junction between cytoplasm or extracellular fluid, with n_D=1.35–1.38, and lipid-rich membranes, with n_D=1.47, in the form of cell borders, cell nucleus membranes, and mitochondrial membranes [77] (Fig. 2.14).

The amount of back-scattered light depends on the structure of the interface surfaces. Rough surfaces scatter light in a broadly diffuse pattern, whereas directed waves with narrow scatter cones are formed on smooth structures. In addition, the confocal image is influenced by the number as well as by the size and orientation of scattering organelles or particles. Objects whose diameters are of the same order of magnitude as the wavelength of the laser light display Mie scatter, and much smaller molecules display Rayleigh scatter, which is directed backward to a greater extent than Mie scatter is. Different orientations of elongated cell organelles can place different particle cross-sections in the path of the incident light beam, the result being that the light is back-scattered to varying degrees. A high proportion of cell organelles also increases the amount of back-scattered light [6, 18].

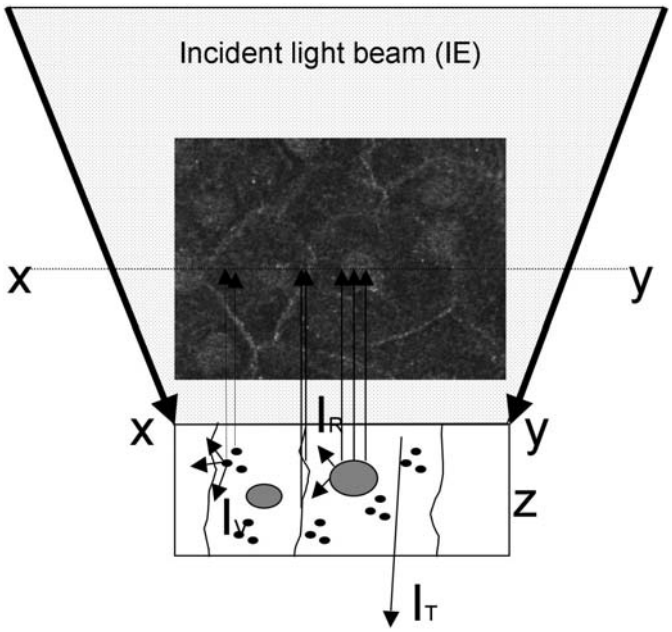

Fig. 2.14 The confocal image of one section (*x, y*) is produced by the sum of the back-scattered light intensities (*Ir*) from the focal depth range (*z*). (*Iv* forward scatter, *It* transmission)

2.4 Noncontact Confocal Laser Scanning Microscopy

Noncontact laser scanning microscopy offers the advantage of contact-free high-resolution imaging of the tear film in particular [79] and also of the posterior corneal structures, such as the keratocytes, and of the endothelium. This becomes especially important in the cellular assessment of surface wound healing.

For noncontact microscopy with the HRT II–RCM, the water-immersion objective with the contact cap is removed and replaced with long focal length dry objectives. As well as imaging

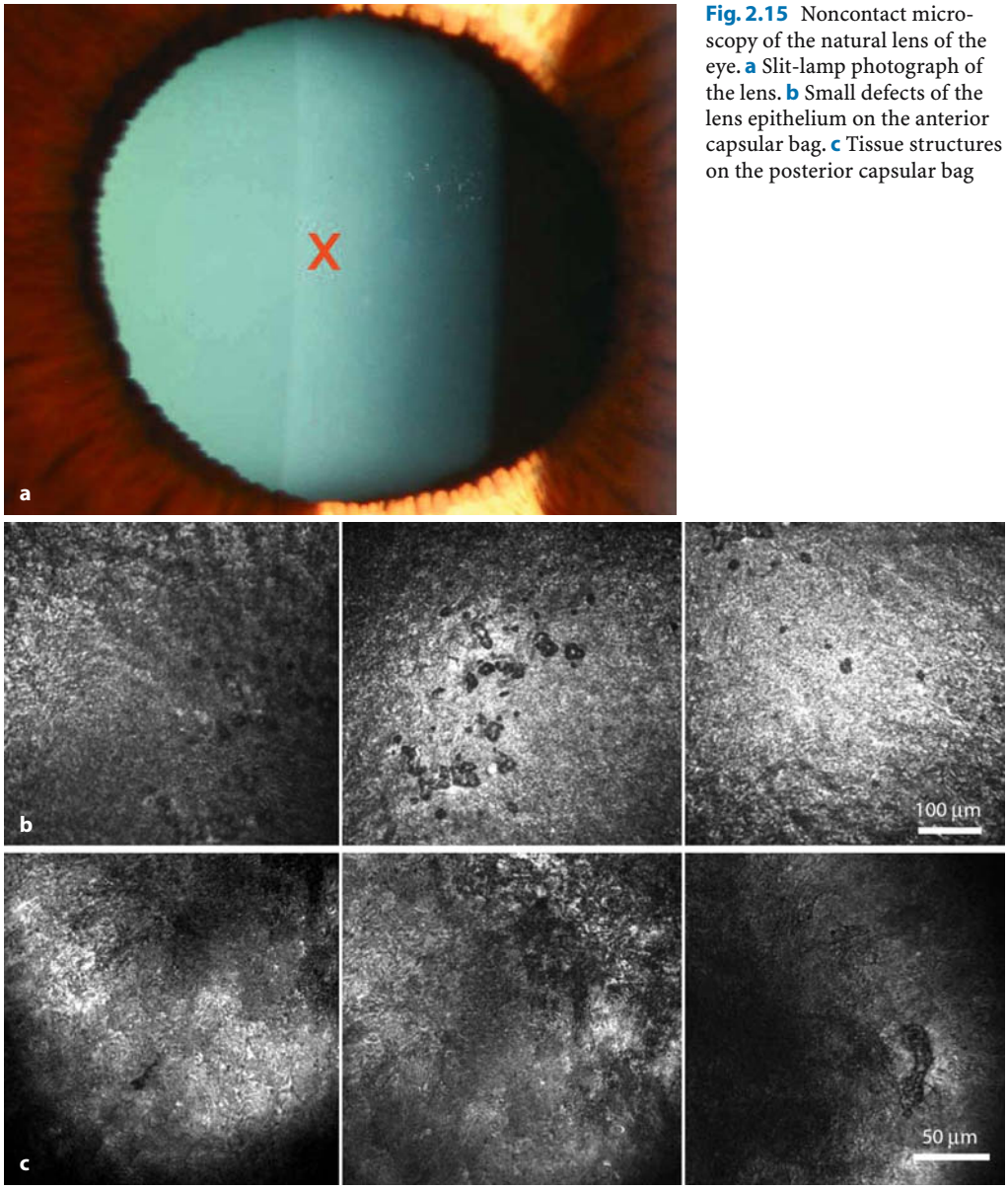

Fig. 2.15 Noncontact microscopy of the natural lens of the eye. **a** Slit-lamp photograph of the lens. **b** Small defects of the lens epithelium on the anterior capsular bag. **c** Tissue structures on the posterior capsular bag

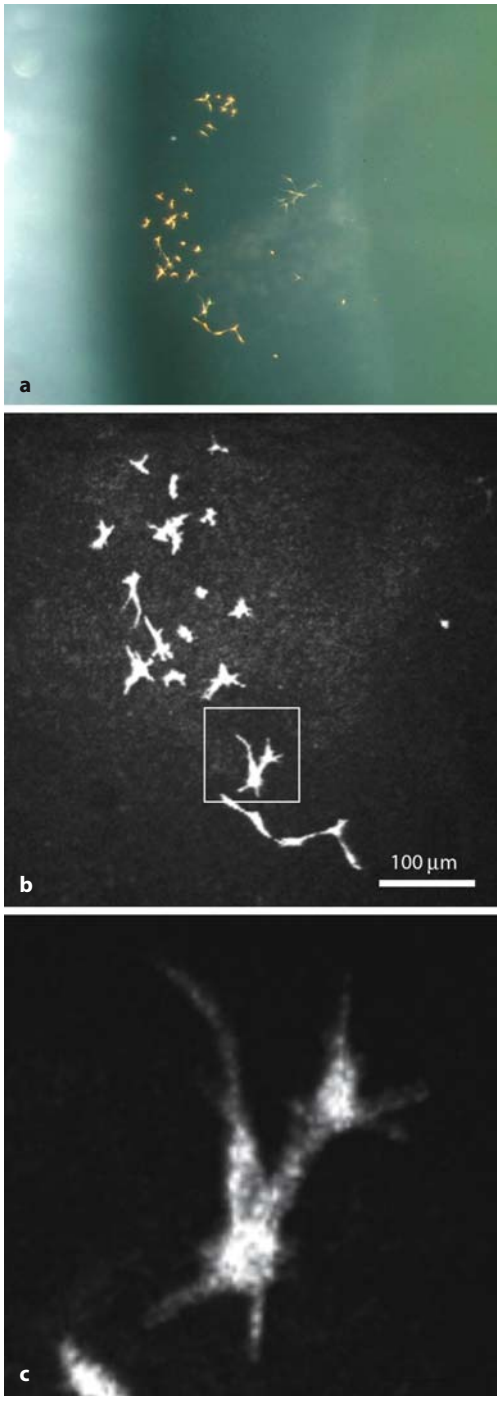

Fig. 2.16 Pigment deposition on the anterior capsular bag. **a** Slit-lamp photograph. **b** Confocal laser scanning microscopy. **c** Higher magnification (manual laser intensity regulation)

the corneal structures mentioned above, it is also possible to perform microscopy of the structures of the natural lens as far as the posterior aspect of the capsule when objectives with super-long focal length and high numeric aperture are used (Fig. 2.15). It is also possible to image secondary cataract formation following intraocular lens implantation.

The dry microscope lens Nikon ×50, 0.45 CF Plan, SLWD (17 mm) in conjunction with the RCM and the HRT II has been found to be most efficient for visualizing corneal structures. To visualize lenses/intraocular lens structures, it is advisable to use the Nikon ×20, 0.35 Plan, ELWD (14 mm) or Nikon ×10, 0.21 L Plan, SLWD (17 mm) because the refraction of the cornea produces additional magnification (Fig. 2.16).

It is necessary to reduce the laser power when imaging the tear film because of its high reflectivity, which causes overmodulation of the HRT II image intensifier. Because the present technical status of the HRT II does not permit this, and a software modification was also unsuccessful in this regard, the use of a detachable neutral glass filter on the dry objective has proved highly effective (Fig. 2.17).

The rapid image sequence with this device also enables dynamic processes to be recorded, such as break-up of the tear film in patients with dry eye or the changes occurring following application of ointments or various medicines, with the ability to determine their retention time in the tear film.

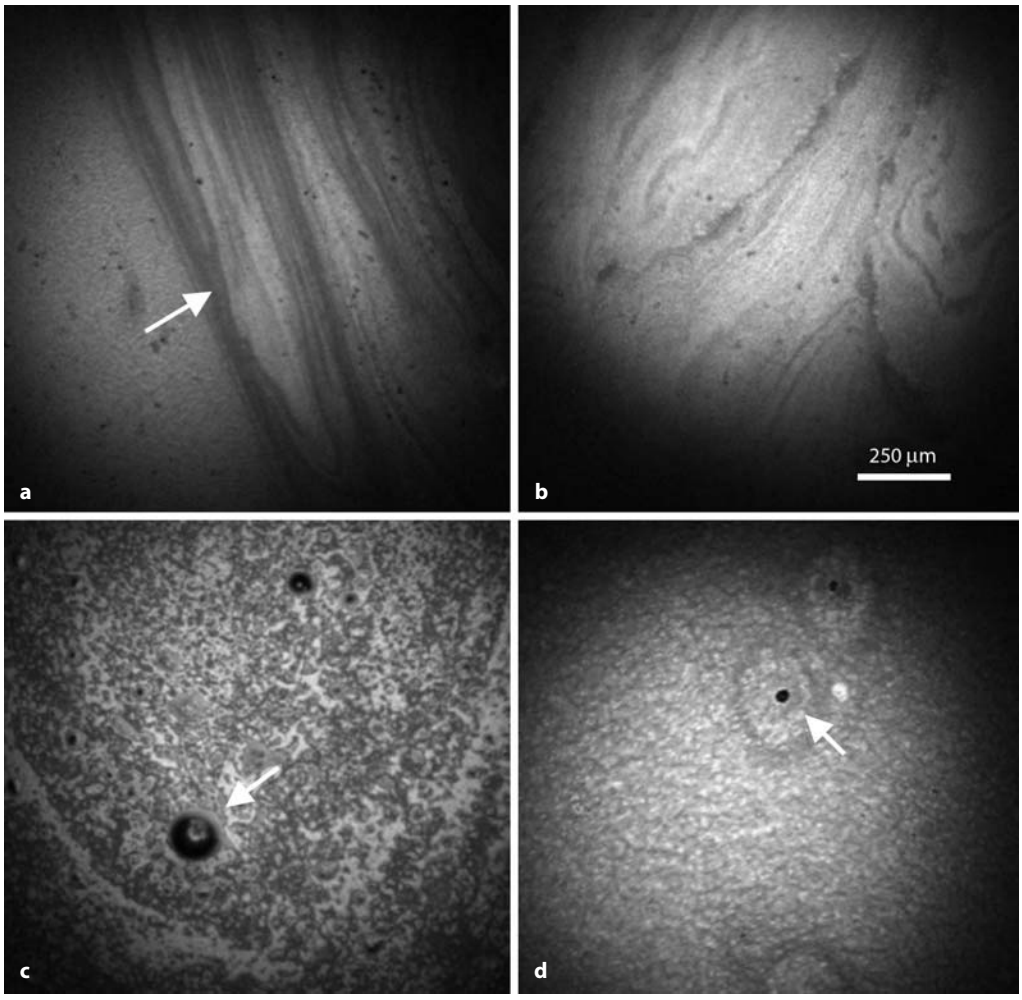

Fig. 2.17 Noncontact laser scanning microscopy of the physiologic tear film. **a, b** Lipid stripes on the tear film after opening the eye. **c** Air bubbles (*arrow*) in the tear film. **d** Meibomian glandular expressions (*arrow*) in the tear film

2.5 Confocal Fluorescence Microscopy

In conventional microscopy, the possibility of using stains to visualize specific anatomical structures provides major information gains. This is particularly true when fluorescence microscopy or immunohistochemistry techniques are used. Because these methods are well-suited for investigating the functional status of tissues ex vivo, they are also of interest for in vivo microscopy. However, problems arise because of the necessity for real-time studies and the selection of suitable nontoxic vital stains. Nevertheless, the first successful steps have already been taken on the road to confocal in vivo fluorescence microscopy of the anterior segments of the eye.

Both the Heidelberg Retina Angiograph (HRA) Classic and the HRA II, which were developed for fluorescence angiography of the ocular fundus, have been modified with the RCM in such a way that this device also permits the

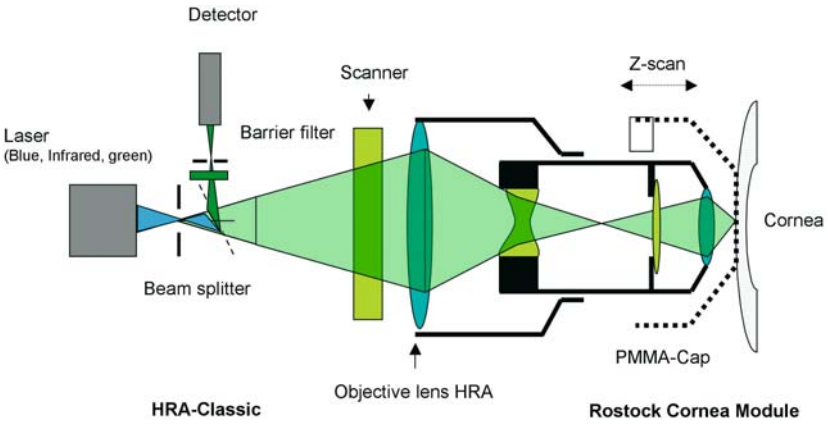

Fig. 2.18 Heidelberg Retina Angiograph (HRA)–Rostock Cornea Module (RCM). Fluorescence mode: *blue* argon laser line. Reflection mode: *green* argon laser line

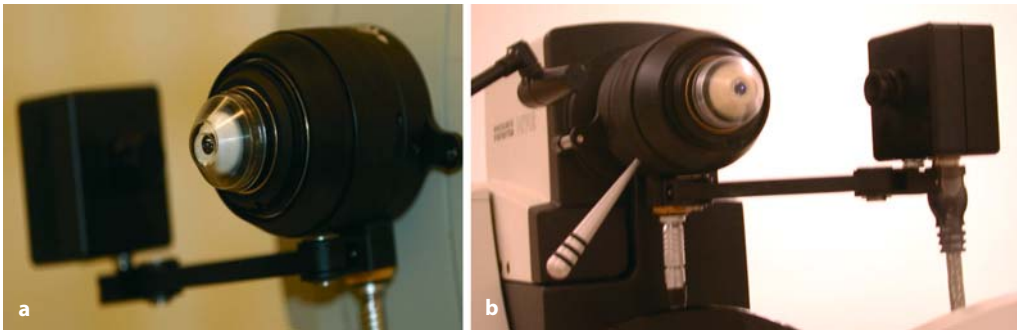

Fig. 2.19 Confocal fluorescence laser scanning microscopes: Rostock Cornea Module (RCM)–Heidelberg Retina Angiograph (HRA) Classic and the HRA II (Heidelberg Engineering, Germany). **a** RCM combined with the HRA Classic (contact). **b** RCM combined with the new fluorescence retina angiograph HRA II (contact)

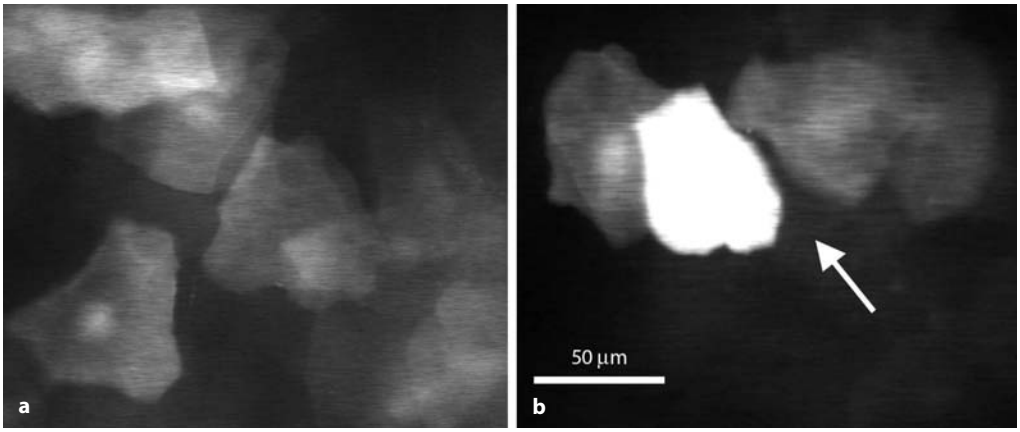

Fig. 2.20 Confocal fluorescence microscopy of the corneal epithelium from a pig's eye (Rostock Cornea Module–Heidelberg Retina Angiograph Classic). **a** Autofluorescence of superficial cells. **b** Fluorescein-stained superficial cell (*arrow*)

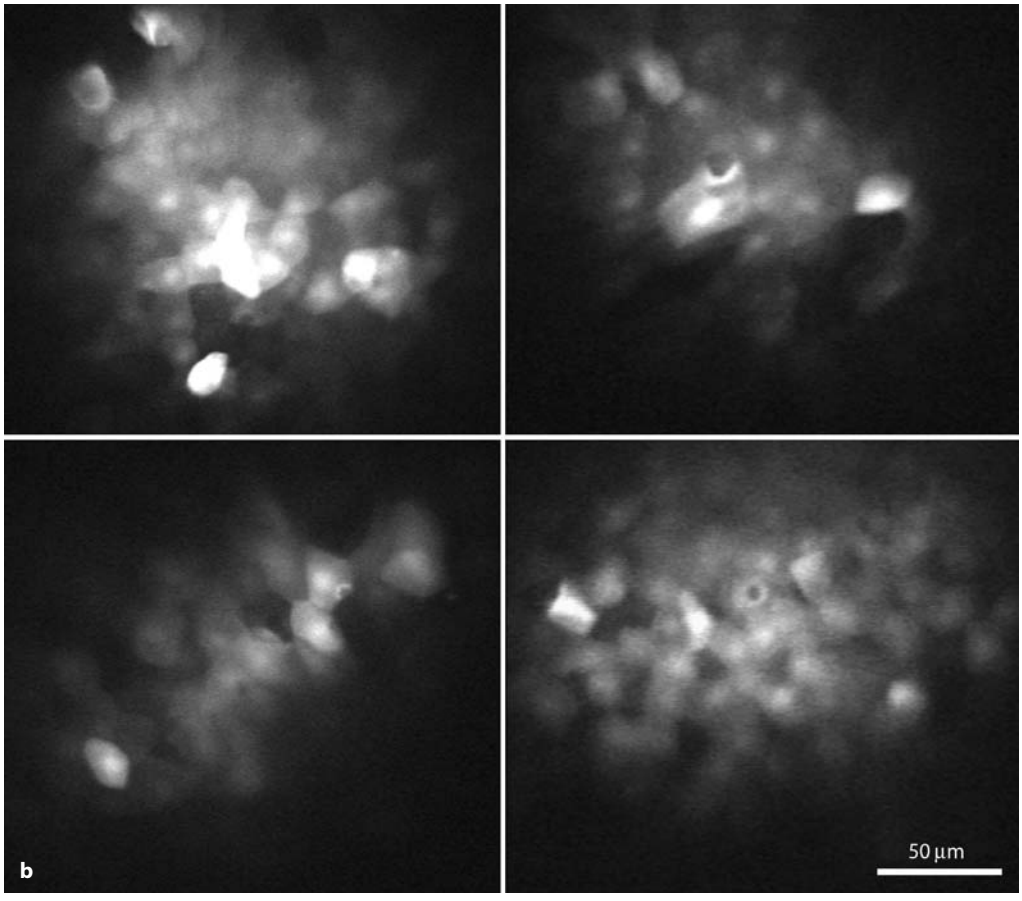

Fig. 2.21 Confocal noncontact fluorescence laser-scanning microscopes [Rostock Cornea Module (RCM)–Heidelberg Retina Angiograph (HRA) II]. **a** RCM (noncontact) adapted for the HRA II. **b** Noncontact micrograph of sodium fluorescein-stained epithelium after laser-assisted in situ keratomileusis (LASIK)

laser focus to be moved to the plane of the anterior segment of the eye. As a result, it becomes possible to visualize cellular structures of the cornea and conjunctiva by recording intrinsic fluorescence or stimulated fluorescence after labeling with sodium fluorescein (NaF).

Figure 2.18 is a schematic illustration of the combined HRA and RCM. Figure 2.19 shows the HRA Classic and its successor, the HRA II, combined with the RCM as a confocal contact microscope.

The functional principle here is the same as with the modification of the HRT II. The wavelength of the integrated argon laser can be switched, for example, with the HRA. As a result, in addition to a reflection image (wavelength

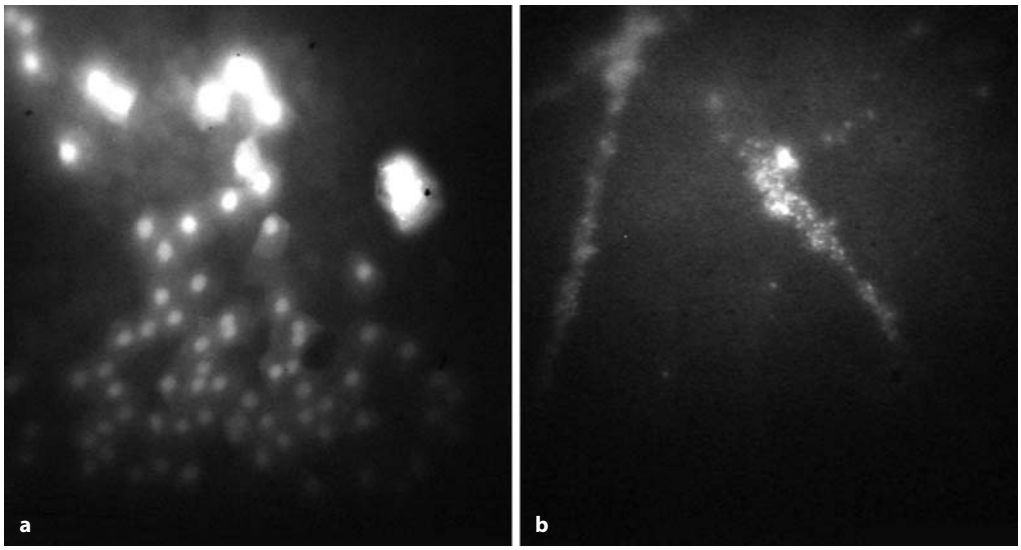

Fig. 2.22 Confocal noncontact fluorescence laser scanning microscopes (Rostock Cornea Module–Heidelberg Retina Angiograph II). **a, b** Epithelium stained with sodium fluorescein (SE Thilo; Alcon, Germany) after mechanical contact with a tonometer system

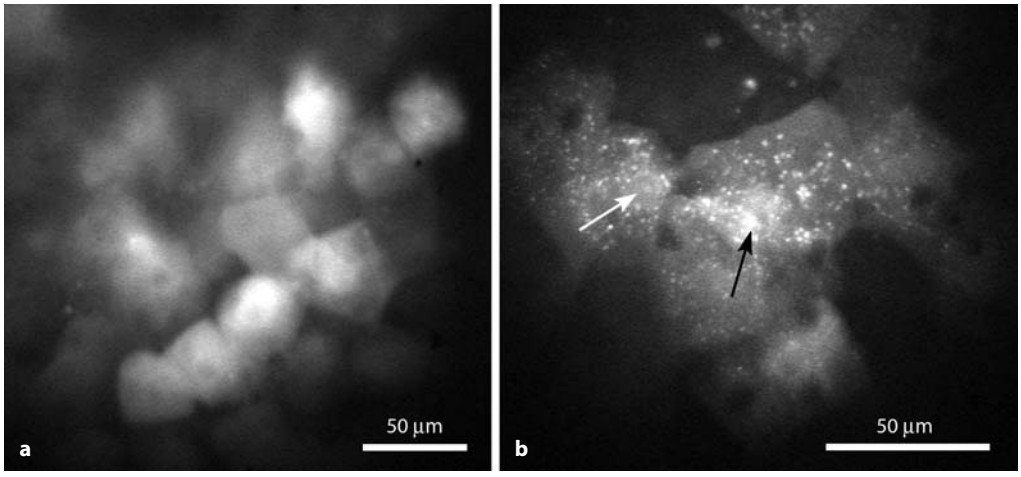

Fig. 2.23 Superficial cells (pig's eye) after pharmacological destruction of the cell membrane and staining with fluorescein (SE Thilo; Alcon, Germany). The fluorescein penetrates the cell membrane (*arrow*) and is concentrated near the nucleus. **a** Untreated. **b** After treatment

514 nm, 150 mW/m²), it is also possible to perform stimulation with blue laser light (wavelength 488 nm, 1.5 W/m²). By adding in a blocking filter (500 nm), it is possible to visualize the fluorescence of NaF-labeled intracellular structures (Figs. 2.20–2.24).

Noncontact fluorescence microscopy utilizes dry objectives with an ultralong working distance (Nikon ×20, 0.35, WD; Nikon ×50, 0.45, WD). For studies using the contact method, a water-immersion objective (×63, Zeiss) is used, which (as in investigations with the HRT II–

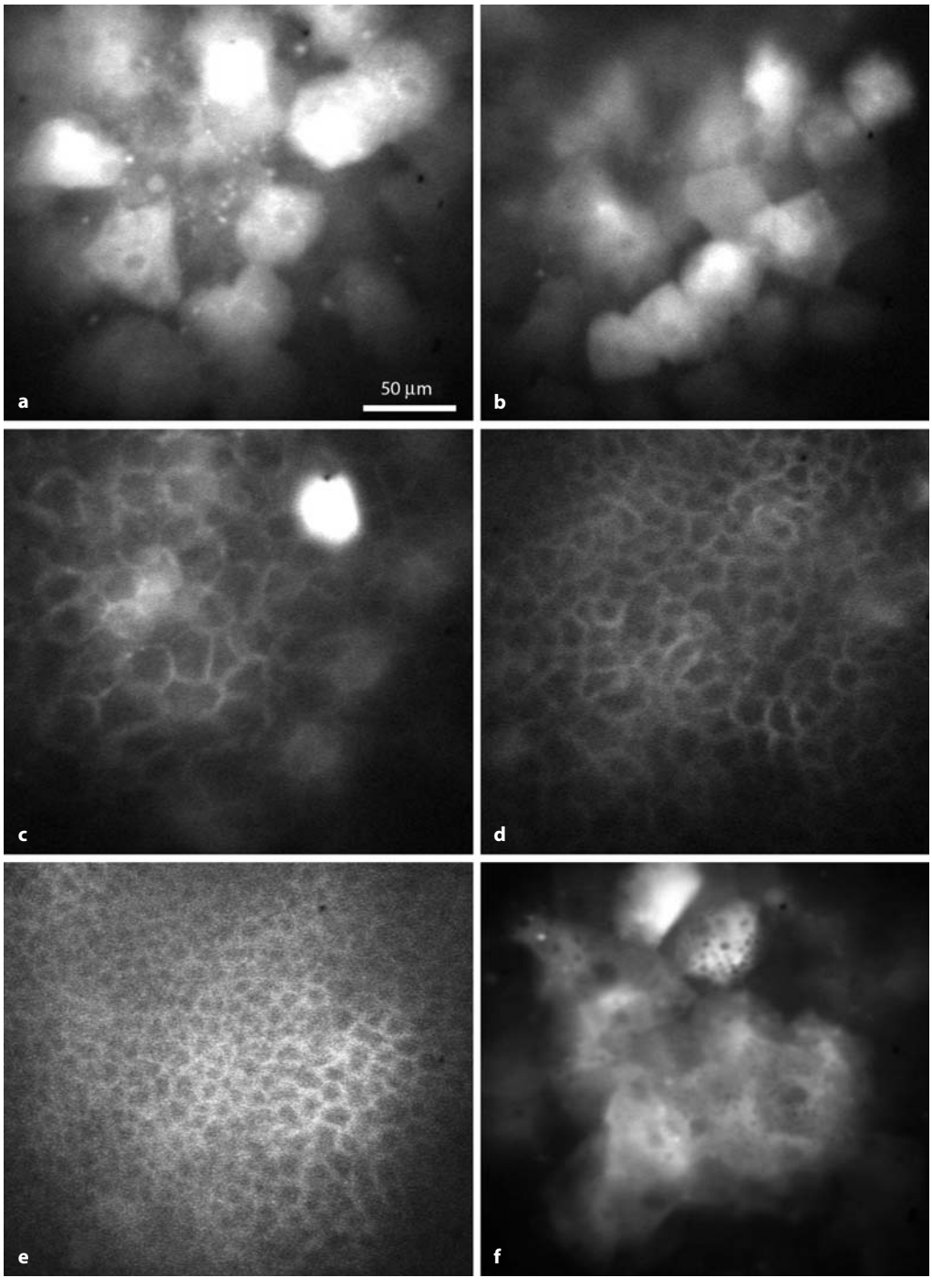

Fig. 2.24 Fluorescein penetration into the cornea: confocal ex vivo contact microscopy with the Rostock Cornea Module–Heidelberg Retina Angiograph II. Porcine cornea following fluorescein staining (Fluo SE Thilo for 1 min; irrigation with 0.9% sodium chloride). **a, b** Superficial cells. **c, d** Intermediate (wing) cells. **e** Basal cells. **f** Superficial cells after 60 min

RCM) is optically coupled to this by the plastic TomoCap® incorporating a plane PMMA disk on the epithelial side and a protective gel (Vidisic). Corneal staining was performed with fluorescein SE Thilo eye drops (Alcon, Germany). Three different magnification stages can be selected (contact methods: 150×150 µm, 250×250 µm, and 400×400 µm; noncontact methods: 450×450 µm, 750×750 µm, and 1,200×1,200 µm). Using this design, it is possible to verify previous findings concerning the staining characteristics and distribution spaces after corneal staining in the in vivo situation.

Figure 2.21 illustrates the HRA II with the RCM as a noncontact fluorescence microscope as well as fluorescence images with varyingly pronounced NaF-stained corneal epithelial cells from a female patient following LASIK surgery. Figure 2.22 shows the epithelium of a patient's eye following multiple contact with a damaged contact cap. Figures 2.23 and 2.24 show ex vivo images of a porcine cornea from a test series following pharmacological lesion induction and staining with fluorescein (Fluorescein SE Thilo, Alcon).